

# A viscoelastic theory of the angular velocity correlation function\*

John A. Montgomery, Jr. and Bruce J. Berne

Department of Chemistry, Columbia University, New York, New York 10027  
(Received 3 August 1976)

Using a frequency-dependent rotational friction coefficient and viscosity, the angular velocity and linear velocity correlation functions are calculated for a spherical test particle in a viscoelastic fluid. The theory is compared with molecular dynamics data using values of the shear viscosity and viscoelastic relaxation time found from kinetic theory and from least squares fits to the data. While good fits are obtained in all cases, the viscosities obtained from fits of the angular velocity correlation function are much smaller than the Enskog values.

## I. INTRODUCTION

In the early work of Stokes<sup>1</sup> and Perrin,<sup>2</sup> the drag forces and torques on a uniformly translating and rotating spheroidal body were computed by solving the Navier–Stokes equations for an incompressible viscous continuum fluid subject to boundary conditions ranging from complete stick to slip in the low Reynolds number limit. The friction constants obtained in this approximation are well-known and have been applied quite successfully to polymer dynamics.

In recent years, it has been shown that these friction coefficients also describe translational and rotational diffusion in simple fluids. For example, Alder, Gass, and Wainwright<sup>3</sup> have shown from a computer simulation of a neat fluid of smooth spheres that the translational friction constant is within machine error  $4\pi\eta a$ , where  $\eta$  is the shear viscosity and  $a$  is the sphere radius. This is precisely the Stokes result for slippery spheres. In addition, Hu and Zwanzig<sup>4</sup> have solved for the drag torque on a uniformly rotating slippery spheroid by using a variational principle. Assuming that benzene is an oblate ellipsoid, their results are in striking agreement with the recent dynamic light scattering results of Bauer *et al.*<sup>5</sup> Recently, this approach has been extended to a more fine grained structure of benzene leading to the expected improvement.<sup>6</sup> On the basis of this, plus much evidence not cited here, it is fair to conclude that molecular hydrodynamics is quite successful for the prediction of certain transport coefficients.

Several years ago, Zwanzig and Bixon<sup>7</sup> generalized a theory of Boussinesq and applied it to a calculation of the velocity autocorrelation function of a particle moving in a neat fluid. In this calculation, the particle translates nonuniformly in a compressible viscoelastic continuum fluid. Zwanzig and Bixon solved the Navier–Stokes equations in the low Reynolds number limit for arbitrary boundary conditions, that is, boundary conditions intermediate between pure slip and pure stick. Using a single viscoelastic relaxation time model, this theory gives qualitative agreement with computer simulations. More recently, Verlet *et al.* have shown that with a two relaxation time model, they can reproduce many of the details of their machine calculations. An interesting feature of the Zwanzig–Bixon model is that it also leads to the correct asymptotic  $t^{-3/2}$  tail observed by Alder and Wainwright.<sup>8</sup>

O’ Dell and Berne<sup>9</sup> have recently studied the rough sphere fluid by computer simulation. They have determined the angular velocity and orientational correlation functions over a wide range of densities, but could not explain their results on the basis of any well-known model. It is therefore of considerable interest to compute the angular velocity autocorrelation function of a sphere in a compressible, viscoelastic fluid and to compare this with molecular dynamics.

## II. HYDRODYNAMIC DRAG FORCE

In this section, we briefly indicate how the hydrodynamic drag on a sphere executing rotational oscillations in a compressible, viscoelastic fluid is found. We resolve the velocity field  $\mathbf{v}(t)$  into its Fourier components  $\mathbf{v}_\omega$ , defined by

$$\mathbf{v}_\omega = \int_{-\infty}^{\infty} dt e^{i\omega t} \mathbf{v}(t).$$

The Navier–Stokes equation satisfied by  $\mathbf{v}_\omega$  is given in convenient form by Zwanzig and Bixon, whose notation

$$\omega^2 \mathbf{v}_\omega + C_1^2 \nabla \nabla \cdot \mathbf{v}_\omega - C_2^2 \nabla \times \nabla \times \mathbf{v}_\omega = 0 \quad (1)$$

we adopt here. We must solve Eq. (1) subject to stick boundary conditions on the surface of the rotating sphere.

We assume the sphere to have radius  $R$  and angular velocity  $\Omega(t)$ , with Fourier components  $\Omega_\omega$ . The velocity field of the fluid must, therefore, satisfy

$$\mathbf{v}_\omega = \Omega_\omega \times \mathbf{R} \quad (2)$$

on the surface of the sphere.

We solve the Navier–Stokes equation using the vector spherical harmonics of Morse and Feshbach, taking  $\Omega_\omega$  along the polar axis. We expand the velocity field as

$$\mathbf{v}_\omega = \sum (A_L \mathbf{L} + A_M \mathbf{M} + A_N \mathbf{N}),$$

where the vector harmonics  $\mathbf{L}$ ,  $\mathbf{M}$ , and  $\mathbf{N}$  are given in Eq. (32) of Zwanzig and Bixon.<sup>7</sup> By symmetry, in spherical coordinates  $\mathbf{v}_\omega$  has no component along the unit vector specifying the direction of  $\theta$ . On the surface of the sphere, the only vector harmonic satisfying the boundary condition Eq. (2) is  $\mathbf{M}_{01}$ , so that the velocity field is given by

$$\mathbf{v}_\omega = A_M \mathbf{M}_{01},$$

or explicitly by

$$\mathbf{v}_\omega = A_M h_1(k_t r) \sin \theta \mathbf{a}_\phi, \quad (3)$$

where  $k_t \equiv i\sqrt{-i\omega\rho/\eta}$  and  $h_1$  is a spherical Hankel function. Matching Eqs. (2) and (3) at  $r=R$  gives

$$A_M = \Omega_\omega \frac{k_t^2 R^2}{i + k_t R} e^{-ik_t R}.$$

This is identical to the incompressible case, as would be expected intuitively because a sphere rotating in its own volume would not excite any longitudinal (sound) modes in the fluid. The drag torque on the sphere is then evaluated from the stress tensor as in Landau and Lifshitz.<sup>11</sup> The result gives a drag torque  $\mathbf{N}_\omega = -\zeta(\omega)\Omega_\omega$  where  $\zeta(\omega)$  is the frequency-dependent rotation friction coefficient

$$\zeta(\omega) = \zeta_R [1 - (k_t R)^2 / 3(1 - ik_t R)]$$

and where  $\zeta_R \equiv 8\pi\eta R^3$  is the static rotational friction coefficient. We find it convenient to use the Laplace transform of the friction coefficient, which is defined by

$$\zeta(p) = \int_0^\infty dt e^{-pt} \zeta(t)$$

and obtained from  $\zeta(\omega)$  by replacing  $-i\omega$  by  $p$ . The result is

$$\zeta(p) = \zeta_R [1 + \alpha^2 p / 3(1 + \alpha\sqrt{p})], \quad (4)$$

where the penetration time  $\alpha^2$  is  $\alpha^2 \equiv \rho_s R^2 / \eta$  and  $\rho_s$  is the fluid density ( $\alpha^2$  is the time required for transverse momentum to diffuse distance equal to the radius of the sphere).

### III. HYDRODYNAMIC ANGULAR VELOCITY CORRELATIONS (AVCF)

The Laplace transform  $\bar{C}(p)$  of the normalized AVCF is found from linear response theory<sup>12</sup> to be

$$\bar{C}(p) = \frac{1}{p + \zeta(p)/I}.$$

It is useful when discussing rotating spheres to define a loading parameter  $\kappa \equiv I/mR^2$ , where  $I$  is the moment of inertia and  $m$  is the mass of the sphere. The parameter  $\kappa$  measures the rotational inertia of the sphere and can vary between  $\kappa = 0$  and  $\kappa = \frac{2}{3}$ , depending on whether the mass is completely concentrated in the center of the sphere or entirely on its surface. Intermediate values of  $\kappa$  correspond to other mass distributions. Another property of importance is the mass density  $\rho$  of the sphere, relative to the mass density  $\rho_s$  of the solvent.

If time is measured in units of the penetration time  $\alpha^2$ , or equivalently  $p$  is measured in units of  $\alpha^{-2}$ , then  $C(p)$  can be expressed as

$$\bar{C}(p) = \frac{1 + p^{1/2}}{p^{3/2} + [(\lambda + 2/\lambda)]p + (6/\lambda)p^{1/2} + 6/\lambda},$$

where  $\lambda$  is a parameter combining the effects of buoyancy and inertia

$$\lambda \equiv \kappa \rho / \rho_s.$$

The denominator can be factored so that

$$\bar{C}(p) = \frac{1 + \sqrt{p}}{(\sqrt{p} + a)(\sqrt{p} + b)(\sqrt{p} + b^*)}, \quad (5)$$

where  $-a$ ,  $-b$ , and  $-b^*$  are the roots of the cubic equation

$$x^3 + \left(\frac{\lambda + 2}{\lambda}\right)x^2 + \frac{6}{\lambda}x + \frac{6}{\lambda} = 0.$$

The Laplace inverse of Eq. (5) is then found to be

$$C(t) = \frac{a(a-1)}{(b-a)(b^*-a)} e^{a^2 t} \operatorname{erfc}(a\sqrt{t}) + 2\operatorname{Re} \frac{b(b-1)}{(b-b^*)(b-a)} e^{b^2 t} \operatorname{erfc}(b\sqrt{t}), \quad (6)$$

where  $\operatorname{erfc}(x)$  is the complimentary error function of  $x$ . A similar result has been reported by Subramanian and Davis.<sup>13</sup>

The extension to viscoelastic behavior is done by substituting a frequency-dependent viscosity  $\eta(p)$  in place of  $\eta$ . The single relaxation time approximation is written

$$\eta(p) = \eta / (1 + \gamma p),$$

where  $\gamma$  is the viscoelastic relaxation time (in units of  $\alpha^2$ ). It is, of course, possible to use more complicated models of viscoelasticity.

The Laplace transform of the AVCF becomes

$$\bar{C}(p) = \frac{\lambda(1 + \gamma p)(1 + \sqrt{A})}{\lambda A^{3/2} + (\lambda + 2)A + 6A^{1/2} + 6}, \quad (7)$$

where  $A \equiv p(1 + \gamma p)$ .  $C(p)$  can be expressed in factored form as

$$\bar{C}(p) = \frac{(1 + \gamma p)(1 + \sqrt{A})}{(\sqrt{A} + a)(\sqrt{A} + b)(\sqrt{A} + b^*)}, \quad (8)$$

where  $a$ ,  $b$ , and  $b^*$  are the same as in Eq. (5). We use the Mellin inversion formula to find  $C(t)$ , noting from Eqs. (7) and (8) that  $\bar{C}(p)$  has branch points at 0 and  $-1/\gamma$  and three poles in the complex  $p$  plane. The integral

$$C(t) = \frac{1}{2\pi i} \int_{-i\infty - \gamma}^{i\infty - \gamma} dp e^{pt} \frac{\lambda(1 + \gamma p)(1 + A^{1/2})}{\lambda A^{3/2} + (\lambda + 2)A + 6A^{1/2} + 6} \quad (9)$$

can be evaluated by closing the contour as indicates in Fig. 1. As  $R \rightarrow \infty$  and  $\epsilon \rightarrow 0$  (see figure), the integral along  $AB$  becomes the integral of Eq. (9). There is no contribution in the limit from the semicircles  $BC$ ,  $DE$ , and  $FA$ . The integrals along  $CD$  and  $EF$  cancel except between the branch points. Separating Eq. (8) by partial fractions to calculate the residues at the three poles and using Eq. (7) to evaluate the integrals along the cut, we have

$$C(t) = \left( \frac{1 - \sqrt{1 + 4\gamma a^2}}{\sqrt{1 + 4\gamma a^2}} \right) \exp\left(-\frac{1 + \sqrt{1 + 4\gamma a^2}}{2\gamma} t\right) + 2\operatorname{Re} \left( \frac{1 - \sqrt{1 + 4\gamma b^2}}{\sqrt{1 + 4\gamma b^2}} \right) \exp\left(-\frac{1 + \sqrt{1 + 4\gamma b^2}}{2\gamma} t\right) + \frac{2\lambda}{\pi} \int_0^{1/\gamma} dx e^{-xt} \times \frac{(1 - \gamma x)[x(1 - \gamma x)]^{3/2}}{[6 - (\lambda + 2)x(1 - \gamma x)]^2 + x(1 - \gamma x)[6 - \lambda x(1 - \gamma x)]^2} \quad (10)$$

Note that as  $\gamma \rightarrow 0$ , the pole terms vanish and Eq. (10)

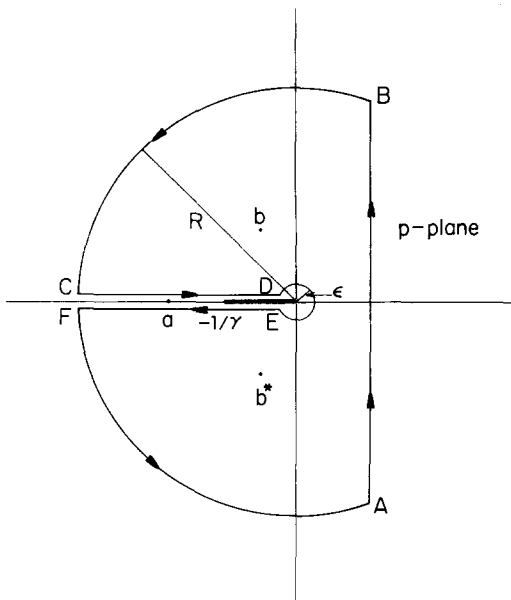


FIG. 1. Contour used for the integral of Eq. (9). The branch cut is indicated by a heavy dark line.

becomes an integral representation of Eq. (6).

#### IV. DECAY OF THE AVCF AT LONG AND SHORT TIMES

In this section we find the limiting behavior of the AVCF at long and short times and compare it with previous results. First consider the behavior of Eq. (10) at  $t \rightarrow \infty$ . Ignoring the pole terms, since their asymptotic behavior is uninteresting, Eq. (10) becomes

$$C(t) = \frac{2\lambda}{\pi t} \int_0^{t/r} dz e^{-z} \times \frac{\left(1 - \frac{\gamma z}{t}\right) \left[\frac{z}{t} \left(1 - \frac{\gamma z}{t}\right)\right]^{3/2}}{\left[6 - (\lambda + z) \frac{z}{t} \left(1 - \frac{\gamma z}{t}\right)\right]^2 + \frac{z}{t} \left(1 - \frac{\gamma z}{t}\right) \left[6 - \frac{\lambda z}{t} \left(1 - \frac{\gamma z}{t}\right)\right]^2},$$

where  $z = xt$ . In the limit  $t \rightarrow \infty$  it is clear that

$$C(t) \rightarrow \frac{2\lambda}{\pi t^{5/2}} \int_0^\infty dz e^{-z} \frac{z^{3/2}}{36} = \frac{\lambda}{24\sqrt{\pi}} \frac{1}{t^{5/2}},$$

where  $t$  is in reduced units. In real time

$$C(t) \rightarrow \frac{\lambda}{24\sqrt{\pi}} \left(\frac{R^2}{\nu t}\right)^{5/2}. \tag{11}$$

This result is in agreement with the asymptotic behavior predicted from generalized hydrodynamics by Ailawadi and Berne<sup>14</sup> and corrects a slight misprint in a previous result given by Berne.<sup>12</sup> Note that viscoelasticity does not alter the long-time behavior of the AVCF.

Now consider the behavior of the AVCF for  $t \ll 1$ . Expanding Eq. (8) to lowest order in  $1/p$  and taking  $p \rightarrow \infty$ , we obtain

$$C(p) \rightarrow \frac{1}{p} - \frac{2}{\lambda\sqrt{\gamma}} \frac{1}{p^2} + O\left(\frac{1}{p^3}\right).$$

Laplace inversion shows that the initial decay of the AVCF is given by

$$C(t) \rightarrow 1 - \frac{2}{\lambda\sqrt{\gamma}} t + O(t^2). \tag{12}$$

Thus, the initial decay of the viscoelastic AVCF is linear. Similarly, the initial decay of the viscous AVCF of Eq. (6) is found by an expansion of Eq. (5):

$$C(p) \rightarrow \frac{1}{p} - \frac{2}{\lambda p^{3/2}} + O\left(\frac{1}{p^2}\right),$$

which gives on inversion

$$C(t) \rightarrow 1 - \frac{4}{\lambda\sqrt{\pi}} \sqrt{t} + O(t). \tag{13}$$

Note that for  $t \ll 1$  this decay is faster than exponential (indeed, at the origin, the viscous AVCF has infinite slope). This clearly shows that viscoelasticity is required if a hydrodynamic theory is to reproduce the linear initial decay required in hard systems.

The initial decay of the AVCF is governed by binary collisions rather than hydrodynamic effects. In an assembly of rough spheres, it follows from the exact collision dynamics that the short-time behavior of the AVCF is<sup>9</sup>

$$C(t) = 1 - \frac{2}{3(k+1)} \frac{t}{t_c} + O(t^2), \tag{14a}$$

where the collision time  $t_c$  is

$$\frac{1}{t_c} = 4\pi\sigma^2 \rho_s g(\sigma) \left(\frac{kT}{\pi m}\right)^{1/2}, \tag{14b}$$

where  $\sigma = 2R$  and  $g(\sigma)$  is the equilibrium radial distribution function at contact between two spheres. Comparing Eqs. (14a) and (12), we find an expression for the viscoelastic relaxation time in terms of the viscosity  $\eta$  and the collision time (in real time):

$$\gamma = \frac{9(\kappa+1)^2}{\kappa^2 \lambda^2} \left(\frac{\eta t_c}{\rho_s R^2}\right)^2. \tag{15}$$

We will return to this point later.

#### V. COMPARISON WITH MOLECULAR DYNAMICS

As a test of the hydrodynamic behavior of the AVCF and VCF, we compare our theory with the molecular dynamics results of O'Dell and Berne<sup>9</sup> for the rough sphere fluid.

Since the present theory has its origin in macroscopic hydrodynamics, it has in it two undetermined parameters—the viscosity and the viscoelastic relaxation time. We have shown previously how the viscoelastic relaxation time can be found for hard systems from the Enskog theory. The Enskog viscosity for the rough sphere fluid has been found by Dahler and co-workers<sup>15,16</sup> to be

$$\eta = \eta^* \left(1 + \frac{5\kappa+2}{5\kappa+5} bng(\sigma)\right)^2 + \frac{1}{10} \rho_s g(\sigma) \frac{7\kappa+4}{\kappa+1} \left(\frac{kT}{\pi m}\right)^{1/2} bng(\sigma),$$

$$\eta^* = \frac{15}{8\sigma^2 g(\sigma)} \frac{(\kappa+1)^2}{6+13\kappa} \left(\frac{mkT}{\pi}\right)^{1/2},$$

$$b = \frac{1}{3} 2\pi\sigma^2, \quad \rho_s = nm.$$

TABLE I. Comparison of Enskog and least squares parameters for the AVCF and VCF.

$\hat{\rho}$	$\beta$ (Enskog)	$\beta$ (fit, AVCF)	$\beta$ (fit, VCF)	$\gamma$ (Enskog, AVCF)	$\gamma$ (fit, AVCF)	$\gamma$ (fit, VCF)
0.100	5.46	0.383	2.13	0.0868	0.128	1.20
0.333	0.855	0.103	0.598	0.0680	0.0909	0.804
0.500	0.597	0.059	0.455	0.0464	0.0639	1.06
0.625	0.536	0.040	0.528	0.0355	0.0449	2.55

Using  $g(\sigma)$  as found by molecular dynamics, we may calculate theoretically the dimensionless parameter

$$\beta = \frac{t_c}{\alpha^2} = \frac{\eta t_c}{\rho R^2},$$

by which we characterize the viscosity in the rough sphere fluid. We have also found  $\beta$  and  $\lambda$  numerically by a least squares fit to the molecular dynamics data. Table I compares the parameters obtained from the Enskog theory with those obtained by least squares. Figures 2 and 3 show the agreement between the molecular dynamics data and the theoretical correlation function obtained by least squares. For  $\hat{\rho} = 0.333$ , molecular dynamics data accurate at longer times were obtained,<sup>17</sup> and the least squares fit to the AVCF is displayed in Fig. 4.

Table I shows reasonable agreement between the least squares and Enskog values of  $\beta$  (note that we did not attempt to calculate  $\gamma$  theoretically for the VCF, since the theoretical VCF does not have the proper initial value). For the AVCF there is reasonable agreement between the Enskog and least squares results for the viscoelastic parameter  $\gamma$  but poor agreement for the viscosity parameter  $\beta$ , the values of from least squares being much smaller than the Enskog values.

If the AVCF is computed using the Enskog initial slope and viscosity, the function so obtained has large unphysical oscillations, seen in Fig. 5. We cannot rule out the possibility that some more sophisticated description of the viscoelastic response might produce agreement with the data using the Enskog viscosity. It is, however, true that the theoretical AVCF does not become asymptotic until a much longer time than required for the theoretical VCF to become asymptotic, as seen in

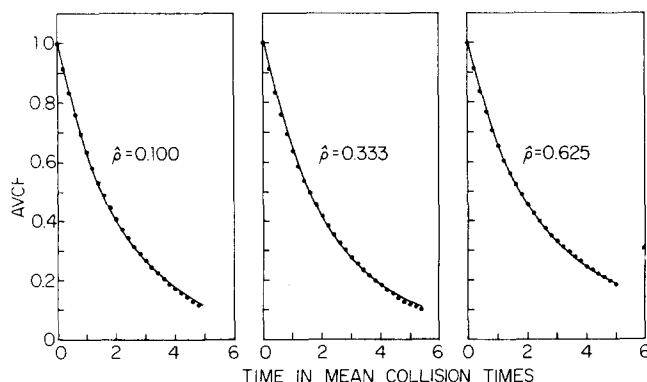


FIG. 2. Comparison of theory and experiment for the AVCF. The points are the molecular dynamics data of O'Dell and Berne, and the solid curve is computed from Eq. (10).  $\hat{\rho} = n\sigma^3/\sqrt{2}$  is the number density relative to closest packing.

Fig. 6. It is therefore clear that it will be very difficult to observe the long time tails in the rotational motion.

## APPENDIX A: VISCOELASTIC THEORY OF THE VELOCITY CORRELATION FUNCTION (VCF)

In this section viscoelasticity is introduced into the Boussinesq friction for a translating particle and the VCF is computed. In a later section this result is compared with the molecular dynamics study of the rough sphere fluid.

The Boussinesq result for the translational friction is<sup>11</sup>

$$\zeta(\omega) = 6\pi\eta R - \frac{2}{3}\pi R^3 i\omega\rho - 6\pi R^2 i\sqrt{i\omega\rho\eta}. \quad (\text{A.1})$$

The Laplace transform  $\zeta(p)$  expressed in our units, is

$$\zeta(p) = \zeta_T [1 + (1/9)p + \sqrt{p}], \quad \zeta_T = 6\pi\eta R.$$

Note that this is the result obtained for stick boundary conditions. Using the viscoelastic model introduced for the AVCF,

$$\zeta(p) = \frac{\zeta_T}{1 + \gamma p} \left( 1 + \sqrt{p(1 + \gamma p)} + \frac{1}{9} p(1 + \gamma p) \right) \quad (\text{A.2})$$

and following a similar development, the Laplace transform of the normalized viscoelastic VCF is found to be

$$\begin{aligned} \tilde{C}_v(p) &= \frac{1}{p + \zeta(p)/m} \\ &= \frac{2\epsilon(1 + \gamma p)}{(2\epsilon + 1)p(1 + \gamma p) + 9\sqrt{p(1 + \gamma p)} + 9}, \end{aligned} \quad (\text{A.3})$$

where  $\epsilon \equiv \rho/\rho_s$ .

We find the inverse Laplace transform by a contour integration, the result is

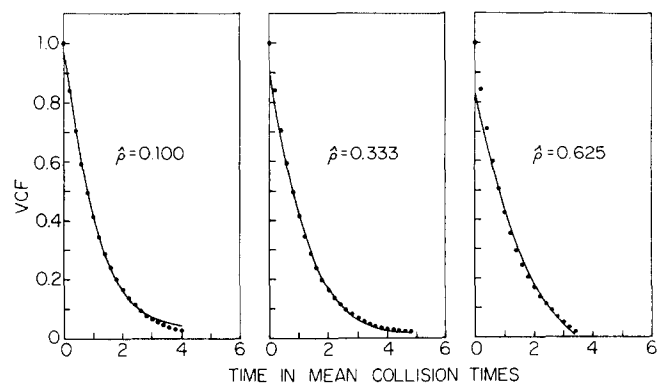


FIG. 3. Comparison of theory and experiment for the VCF. The points are the molecular dynamics data of O'Dell and Berne, and the solid curve is computed from Eq. (A.4).

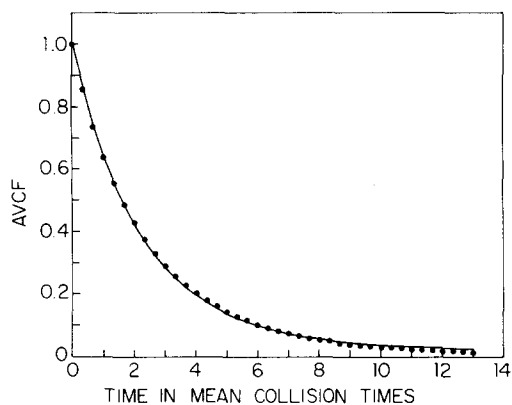


FIG. 4. Comparison of theory and experiment for the AVCF at long times  $\hat{\rho}=0.333$ .

$$C_v(t) = \frac{2t}{2\epsilon + 1} \left[ \frac{a_+}{\sqrt{1+4\gamma a_+^2}} (1 - \sqrt{1+4\gamma a_+^2}) \exp\left(-\frac{1+\sqrt{1+4\gamma a_+^2}}{2\gamma} t\right) + \frac{a_-}{\sqrt{1+4\gamma a_-^2}} (1 + \sqrt{1+4\gamma a_-^2}) \exp\left(-\frac{1+\sqrt{1+4\gamma a_-^2}}{2\gamma} t\right) \right] + \frac{18\epsilon}{\pi} \int_0^{1/\gamma} dx e^{-xt} \frac{\sqrt{x}(1-\gamma x)^{3/2}}{[g - (2\epsilon + 1)x(1-\gamma x)]^2 + 81x(1-\gamma x)} \quad (A.4)$$

where  $a_{\pm}$  are given by

$$a_{\pm} = \frac{9}{2(2\epsilon + 1)} \left[ 1 \pm \sqrt{1 - \frac{4}{9}(2\epsilon + 1)} \right].$$

Note that this correlation function has an initial value less than unity, reflecting the fact that a particle in an incompressible fluid translates with an effective mass  $M^* = M + \frac{2}{3}\rho_s\pi R^3$ . A similar result is given by Chow<sup>15</sup> (whose result corresponds to replacing  $M^*$  by  $M$  in the above equations). It should be noted that the long and short time limits of the viscoelastic VCF are found to be (in real time)

$$C_v(t) \xrightarrow[t \rightarrow \infty]{} \frac{\epsilon}{9\sqrt{\pi}} \left( \frac{R^2}{\nu t} \right)^{3/2} \quad (A.5)$$

and

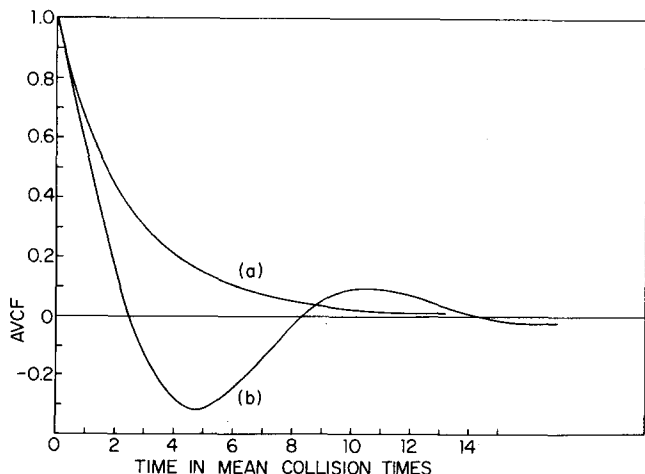


FIG. 5. Curve (a) is the least squares AVCF for  $\hat{\rho}=0.333$ . Curve (b) is the AVCF with Enskog initial slope and viscosity.

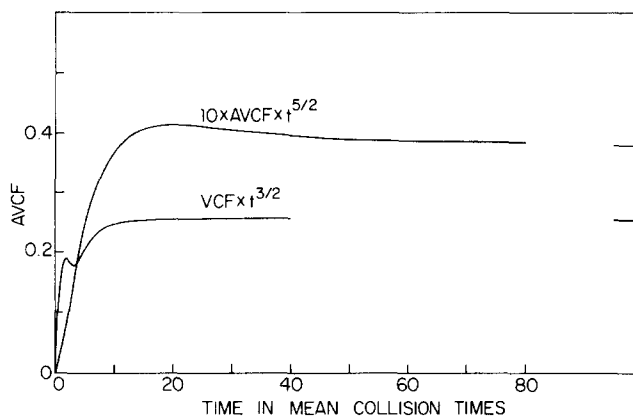


FIG. 6. Asymptotic behavior of the least squares VCF and AVCF.

$$C_v(t) \xrightarrow[t \rightarrow 0]{} \frac{2\epsilon}{2\epsilon + 1} \left( 1 - \frac{9}{2\epsilon + 1} \frac{t}{\sqrt{\gamma}} \right) + O(t^2). \quad (A.6)$$

As expected, our asymptotic decay is in agreement with the results of Ernst, Hague, and van Leeuwen<sup>19</sup> and Dorfman and Cohen.<sup>20</sup> Note that for short times the viscous VCF (obtained when  $\gamma \rightarrow 0$ ) is to lowest order

$$C_v(t) \xrightarrow[t \rightarrow 0]{} \frac{2\epsilon}{2\epsilon + 1} \left( 1 - \frac{18}{(2\epsilon + 1)\sqrt{\pi}} \sqrt{t} + O(t) \right).$$

Once again, a purely viscous model does not give the required linear initial decay.

\*This work is supported by grants from NSF and from NIH.  
<sup>1</sup>G. G. Stokes, *Trans. Camb. Phil. Soc.* **9**, 8 (1851).  
<sup>2</sup>F. Perrin, *J. Phys. Rad.* **5**, 497 (1934); **7**, 1 (1936).  
<sup>3</sup>B. J. Alder, D. M. Gass, and T. E. Wainwright, *J. Chem. Phys.* **53**, 3813 (1970).  
<sup>4</sup>C. M. Hu and R. Zwanzig, *J. Chem. Phys.* **60**, 4354 (1974).  
<sup>5</sup>D. R. Bauer, J. I. Brauman, and R. Pecora, *J. Am. Chem. Soc.* **96**, 6840 (1974).  
<sup>6</sup>G. K. Youngren and A. Acrivos, *J. Chem. Phys.* **63**, 3846 (1975).  
<sup>7</sup>R. Zwanzig and M. Bixon, *Phys. Rev. A* **2**, 2005 (1970).  
<sup>8</sup>B. Alder and T. Wainwright, *Phys. Rev. Lett.* **18**, 968 (1967).  
<sup>9</sup>J. O'Dell and B. J. Berne, *J. Chem. Phys.* **63**, 2376 (1975).  
<sup>10</sup>P. M. Morse and H. Feshbach, *Methods of Theoretical Physics* (McGraw-Hill, New York, 1953).  
<sup>11</sup>L. D. Landau and E. M. Lifshitz, *Fluid Mechanics* (Pergamon, London, 1959).  
<sup>12</sup>B. J. Berne, *J. Chem. Phys.* **56**, 2164 (1972).  
<sup>13</sup>G. Subramanian and H. T. Davis, *Phys. Rev. A* **11**, 1430 (1975).  
<sup>14</sup>N. K. Ailawadi and B. J. Berne, IUPAP Conference on Statistical Physics, Chicago, 1971.  
<sup>15</sup>B. J. McCoy, S. I. Sandler, and J. S. Dahler, *J. Chem. Phys.* **45**, 3485 (1966).  
<sup>16</sup>M. Theodosopulu and J. S. Dahler, *J. Chem. Phys.* **60**, 4048 (1974).  
<sup>17</sup>J. O'Dell (private communication).  
<sup>18</sup>T. S. Chow, *J. Chem. Phys.* **61**, 2868 (1974).  
<sup>19</sup>M. H. Ernst, E. H. Hague, and J. M. J. van Leeuwen, *Phys. Rev. Lett.* **25**, 1259 (1970).  
<sup>20</sup>J. R. Dorfman and E. G. D. Cohen, *Phys. Rev. Lett.* **25**, 1257 (1970).